

Magnetic plasmon hybridization and optical activity at optical frequencies in metallic nanostructures

H. Liu,¹ D. A. Genov,¹ D. M. Wu,¹ Y. M. Liu,¹ Z. W. Liu,¹ C. Sun,¹ S. N. Zhu,² and X. Zhang^{1,*}

¹5130 Etcheverry Hall, Nanoscale Science and Engineering Center, University of California, Berkeley, California 94720-1740, USA

²Department of Physics, National Laboratory of Solid State Microstructures, Nanjing University, Nanjing 210093, People's Republic of China

(Received 30 June 2007; published 14 August 2007)

The excitation of optical magnetic plasmons in chiral metallic nanostructures based on a magnetic dimer is studied theoretically. Hybridization of the magnetic plasmon modes and a type of optical activity is demonstrated at near-infrared frequencies. A linearly polarized electromagnetic wave is shown to change its polarization after passing through an array of magnetic dimers. The polarization of the transmitted wave rotates counterclockwise at incident light frequencies corresponding to the low energy and clockwise at the high energy magnetic plasmon state. A metamaterial made of a large number of coupled magnetic dimers could be utilized as a tunable optically active medium with possible applications in optical elements and devices.

DOI: [10.1103/PhysRevB.76.073101](https://doi.org/10.1103/PhysRevB.76.073101)

PACS number(s): 78.20.Ci, 73.20.Mf, 78.20.Bh

In 1999, Pendry *et al.* reported that a nonmagnetic metallic element, referred to as double split ring resonator (DSRR), with size smaller than the wavelength of radiation, exhibits a strong resonant response to the magnetic component of an incident electromagnetic field.¹ In such systems, there are no free magnetic poles, however, the excitation of displacement currents in the DSRR results in induction of a magnetic dipole moment that is comparable to a bar magnet. Similarly to the electric plasmons (EPs) excited in nanosize particles, an effective media made of DSRRs could support magnetic plasmon (MP) oscillations at GHz frequency, which can be used as frequency selective devices at microwave.² Combined with an electric response that has negative permittivity, such a system could ultimately lead to development of metamaterials with effective negative indexes of refraction.^{3,4} It was also suggested that a combination of magnetic response and chirality could be used as an alternative route to negative refraction.⁶ Various electromagnetic chiral structures have been reported in the microwave spectral range, such as helical wire spring,⁵ swiss-role metal structure,⁶ and rotating rosette shape.^{7,8} Optical activity was also found in fractal aggregates of nanoparticles, where broad spectral response could be achieved due to the self-similarity of the underlying structure.⁹ Recently, metallic elements have been demonstrated, with magnetic response in the near-infrared and visible spectral region.¹⁰⁻¹⁷ This provides new possibilities to engineer magnetically coupled systems and realize artificial chiral effect at optical frequency.

On the other hand, it was shown that the calculation of the resonances modes of a complex metallic nanosize system is equivalent to estimating the electromagnetic interactions in nanostructures of simpler geometry.¹⁸⁻²⁴ The resonances of intricately shaped nanoparticles constitute hybridization states similar to the energy states of molecular systems. Thus, the hybridization principle could provide a simple conceptual approach for the rational design of nanostructures with desired plasmon resonances. This method has already been successfully used to describe the plasmon resonance in nanoshell,^{18,19} nanoparticle dimer,²⁰ nanoshell dimer,^{21,22} and nanoparticle and/or metallic surfaces.^{23,24}

In this paper we introduce a hybridization model to inves-

tigate the magnetic response of a subwavelength nanostructure, referred to as a magnetic dimer (MD). The magnetic dimer consists of two single split-ring resonators (SSRR) coupled through magnetic induction. The fundamental MD resonances are viewed as bonding and antibonding combinations of individual SSRRs eigenmodes. A type of optical activity is observed in the coupled system which is not an inherent property of the individual magnetic resonators. For instance, a linearly polarized light flips into an elliptically polarized state as it passes through an array of magnetic dimers. Overall, all types of wave polarization are accessible with the proposed magnetic plasmon (MP) based metamaterial.

In Fig. 1(a), we present the general configuration of a MD, made of two SSRRs separated by a finite distance D . The slits in the rings are positioned perpendicular to each other, thus providing the platform for a unique set of physical phenomena to take place as discussed below. All characteristic system sizes are provided in the figure with D varying from 100 nm up to 600 nm. A second nanostructure, comprised of magnetic dimers positioned in a planar square array, is depicted in Fig. 1(b). The lattice period is set at 800 nm, and the incident electromagnetic radiation is assumed normal to the x - y plane.

To study the magnetic response of the above described systems, we introduce a MP hybridization model similar to that proposed in the case of EP.¹⁸⁻²⁴ In our approach we use the Lagrangian formalism, first calculating the magnetic energy of a single SSRR and later expanding the theory for a system of resonators. For simplicity, in the analysis we view the SSRR as an ideal LC circuit, composed of a magnetic loop (the metal ring) with inductance L and a capacitor with capacitance C (corresponding to the gap). The resonance frequency of the structure is well known $\omega_0 = 1/\sqrt{LC}$, and the magnetic moment of the SSRR originates from the oscillatory behavior of the currents induced in the resonator. If we define the total charge Q accumulated in the slit as a generalized coordinate, the Lagrangian corresponding to a single SSRR is written as $\mathcal{T} = L\dot{Q}^2/2 - Q^2/2C$, where \dot{Q} is the induced current, $L\dot{Q}^2/2$ relates to the kinetic energy of the oscillations, and $L\omega_0^2 Q^2/2$ is the electrostatic energy stored

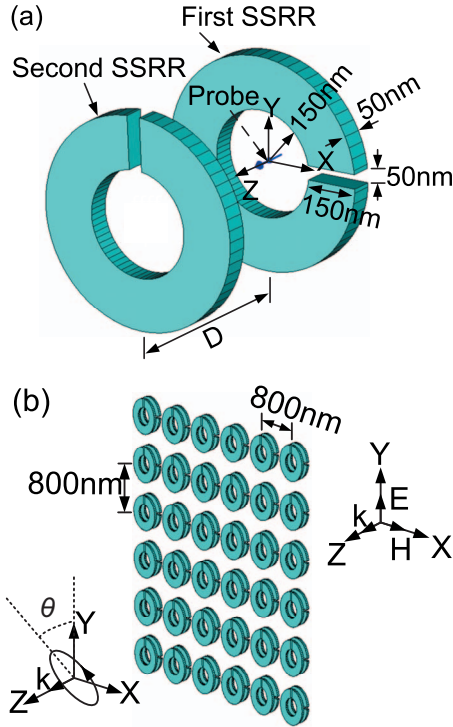


FIG. 1. (Color online) (a) Structure of a single magnetic dimer and (b) chiral metamaterial made of identical dimer elements. All sizes characterizing the system and the direction and polarization of the incident light are shown.

in the SSRR's gap. Similarly, the Lagrangian that describes the MD is a sum of the individual SSRR contributions with added interaction term

$$\mathcal{J} = (L/2)(\dot{Q}_1^2 - \omega_0^2 Q_1^2) + (L/2)(\dot{Q}_2^2 - \omega_0^2 Q_2^2) + M\dot{Q}_1\dot{Q}_2, \quad (1)$$

where Q_i ($i=1,2$) are the oscillatory charges and M is the mutual inductance. By substituting \mathcal{J} in the Euler Lagrange equations

$$(d/dt)(\partial\mathcal{J}/\partial\dot{Q}_i) - \partial\mathcal{J}/\partial Q_i = 0 \quad (i=1,2), \quad (2)$$

it is straightforward to obtain the magnetic plasmon eigenfrequencies $\omega_{\pm} = \omega_0 / \sqrt{1 \mp \kappa}$, where $\kappa = M/L$ is a coupling coefficient. The high energy or antibonding mode $|\omega_+\rangle$ is characterized by antisymmetric charge distribution ($Q_1 = -Q_2$), and the opposite is true for the bonding or low energy $|\omega_-\rangle$ magnetic resonance ($Q_1 = Q_2$). Naturally, the frequency split $\Delta\omega = \omega_+ - \omega_- \approx \kappa\omega_0$ is proportional to the coupling strength.

The Lagrangian (hybridization) formalism provides a phenomenological picture of the electromagnetic response of the system. To study quantitatively the resonance behavior, and check the model, we rely on a set of finite-difference time-domain (FDTD) numerical simulations using a commercial software package, CST Microwave Studio (Computer Simulation Technology GmbH, Darmstadt, Germany). In the calculations, the metal permittivity is given by the Drude model; $\epsilon(\omega) = 1 - \omega_p^2 / (\omega^2 + i\omega\tau)$, where ω_p is the bulk

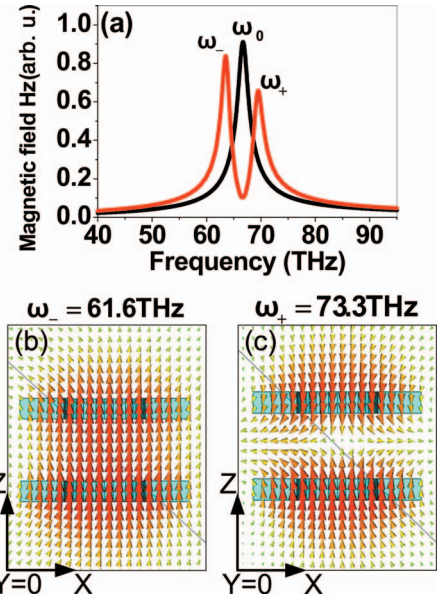


FIG. 2. (Color online) (a) Local magnetic field as detected at the center of a single SSRR (black line), and a magnetic dimer with $D=250$ nm [gray (red) line]. A split in the magnetic resonance is observed due to inductive coupling. The local magnetic field profiles for the (b) bonding and (c) antibonding MP modes are depicted with the symmetric and antisymmetric field distributions are clearly seen.

plasma frequency and ω_τ is the relaxation rate. For gold, the characteristic frequencies, fitted to experimental data, are $\omega_p = 1.37 \times 10^4$ THz and $\omega_\tau = 40.84$ THz.²⁵

For excitation of the magnetic dimer (MD) we use a plane wave, with \vec{E} field polarized in y direction and \vec{H} field in x direction, as shown in Fig. 1(a). For a normal incidence, the magnetic field vector is in the plane of the SSRRs and direct magnetic response is unattainable. However, the electric component of the incident field excites an electric response in the slit and thus a magnetic field could be indirectly induced.¹¹ To study the local magnetic field we position probes at the center of the first SSRR, and vary the incident frequency. The recorded magnetic response is shown in Fig. 2 where the distance between the resonators is set at $D = 250$ nm. As expected, two distinctive resonances with eigenfrequencies $\omega_- = 61.6$ THz and $\omega_+ = 73.3$ THz are recorded. The magnetic response of the constituent SSRR is also depicted, showing a fundamental resonance at $\omega_0 = 66.7$ THz.

The hybridization of the magnetic response in the case of a dimer is mainly due to inductive coupling between the SSRRs. If each SSRR is regarded as a quasiatom, then the MD can be viewed as a hydrogenlike quasimolecule with energy levels ω_- and ω_+ originating from the hybridization of the original (decoupled) state ω_0 . The strength of the inductive coupling depends strongly on the distance between the quasiatoms and for the considered geometry is estimated as $\kappa \approx 0.17$. The specific nature of the MP eigenmodes is studied in Fig. 2 where the local magnetic field distributions in y -cut planes are depicted for the low energy ω_- and high energy ω_+ states, respectively. In accordance to the prediction based on the Lagrangian approach the SSRRs oscillates

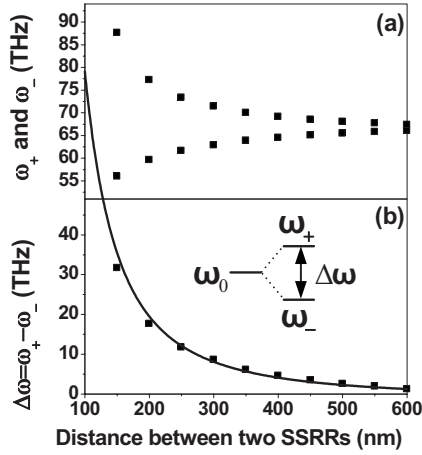


FIG. 3. The dependence of (a) the resonance frequencies ω_{\pm} and (b) the frequency gap $\Delta\omega$ on the distance D between the constituent SSRRs. The frequency gap predicted by the hybridization model (solid line) follows very well the FDTD result (dots). A diagram showing the energy states of the equivalent quasimolecule is included as an inset.

in phase for the bonding mode $|\omega_- \rangle$, and out of phase for the antibonding mode $|\omega_+ \rangle$. Additional information on the eigenmodes magnetic field configuration is given in the supplementary material.²⁸

Since the mutual inductance M decreases dramatically with distance, one should expect a strong change in the resonance frequencies ω_{\pm} . This phenomenon is demonstrated in Fig. 3, where MP eigenfrequencies ω_{\pm} and the frequency change $\Delta\omega = \omega_+ - \omega_-$ are calculated. With decreasing separation between the SSRR an increase in the frequency gap $\Delta\omega$ is observed. The opposite effect takes place at large distances where the magnetic response is decoupled. The specific profile of the frequency gap could be explained by estimating the self- and mutual inductance of the SSRRs: $\Delta\omega \approx \omega_0 \kappa = \omega_0 M/L \propto \int_0^{\infty} dk e^{-kD} J_1^2(kR)$, where R is the SSRR's radius.²⁷ For $D > 2R$, we can expand the integral in series and write $\Delta\omega \propto (R/D)^3 - 3(R/D)^5 + 9.38(R/D)^7$. As evident from Fig. 3(b), this approximated relationship, based on the hybridization method, fits the numerical data quite well.

It is important to mention that the SSRR's size and shape, considered here, have been chosen in order to optimize the magnetic response and allow for a successful nanofabrication. There are several ways to tune the MP properties of the structure, with geometrical modifications having the most significant effect on the MP resonances. For instance, scaling down the size of the resonator R increases the resonance frequency $\omega_0 = 1/\sqrt{LC} \sim 1/R$ due to a linear increase of the inductance $L \sim R$ and capacitance $C \sim R$. However, the kinetic energy of the electrons in the metal is no longer negligible in the infrared range and results in saturation of the magnetic resonance frequency at about 400 THz for noble metals.¹⁴ Another way to tune the resonance is to use different materials, both metals and insulators. For instance, encapsulating the MDs with high index materials cause redshift of the magnetic resonances (for $D=250$ nm and $\epsilon=2$, $\omega_- = 43.3$ THz and $\omega_+ = 51.5$ THz). However, our studies show that optimal magnetic dipole moment is achieved for silver-air or gold-air systems (due to the relatively low intrinsic loss) and a circular shaped SSRR.

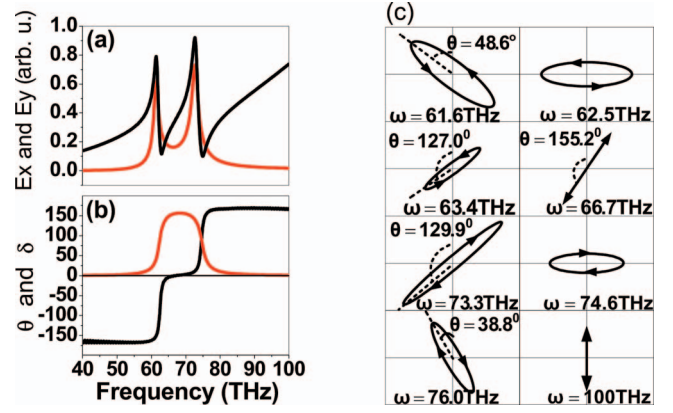


FIG. 4. (Color online) (a) Electric field amplitudes $|E_x|$ [gray (red) line] and $|E_y|$ (black line) for a plain wave passing through a metamaterial made of magnetic dimers. (b) The phase difference δ between the E_y and E_x components of the transmitted wave, and the angle θ between the major polarization axes of the incident and transmitted radiation are also shown with black and gray (red) solid curves, respectively. (c) Polarization states acquired by a plain wave of frequency ω passing through a metamaterial made of periodically arranged MDs ($D=250$ nm).

Having determined the fundamental response of the proposed MD, next we study the propagation of electromagnetic (EM) wave in a metamaterial composed of periodically arranged elements [see Fig. 1(b)]. A plain EM wave is incident on the system and the amplitude and phase change of the transmission wave is detected in far field as shown in Figs. 4(a) and 4(b). The host media is assumed to be air but other dielectric materials such as glass may also be applied. Although the incident light is linearly polarized ($\vec{E} = E_y \hat{y}$), the transmission wave is found to acquire both x and y electric field components in the resonance frequency range and some phase difference between the two orthogonal components. This change in polarization and phase delay originates from the specific three dimensional (3D) chiral arrangement of two SSRRs [see Fig. 1(a)]: one SSRR is shifted a distance from the other and rotates 90° . The electric field in the slit of the first SSRR is aligned along the y axis, and thus a y polarized incident wave is electrically coupled into the system. At resonance, strong magnetic interaction between the SSRRs helps to transfer the energy from the front resonator to the back SSRR. Since the electric field in the slit gap of the second SSRR is along \hat{x} , the electric dipole radiation carries the same polarization. Thus the transmitted wave, detected in far field, is a superposition of x and y polarized light. Unlike the transmission minimum in a waveguide, the E_y appears as a Lorentz line shape around the resonances, which is a typical resonant scattering in free space. On the other hand E_x reaches maximum at the resonance range and becomes zero for off-resonance frequencies due to the diminishing coupling between the SSRRs. According to the classic model developed by Born and Kuhn,²⁶ two spatially separated coupled oscillators, with a chiral symmetry, will induce optical activity for an impinging EM wave. In our system, the hybridization of the MP states constitutes a mechanism for achieving optical activity in the near-infrared range, thus opening opportunities for designing chiral metamaterials. Actually,

Pendry's DSRR structure was also reported to be able to excite two orthogonal polarization states simultaneously,² but it is a planar achiral structure and the necessary retardation effect for optical activity²⁶ is absent, thus it cannot be considered as optically active elements.

The polarization states accessible with the proposed chiral media are presented in Fig. 4(b) where the phase difference δ between the components of the electric field is calculated for the transmitted wave. Remarkably δ undergoes a steplike type of behavior, flipping from -165° to 0° at ω_- and again from 0° to 165° at ω_+ . The change in polarization is easily understood by observing the time evolution of the end point of the electric field vector as it travels through space. For an observer facing the approaching wave, the track of the end point is described by the well known relationship²⁷

$$\left(\frac{E_x}{|E_x|}\right)^2 + \left(\frac{E_y}{|E_y|}\right)^2 - \frac{2E_x E_y}{|E_x||E_y|} \cos \delta = \sin^2 \delta. \quad (3)$$

The polarization state of the EM wave is thus determined by δ , with the end point of the electric field revolving in a clockwise direction for $\sin \delta > 0$ and in a counterclockwise direction for $\sin \delta < 0$. Concurrently for $\omega < \omega_0$, the transmitted wave has right-hand polarization and the dimer constitutes an isomer of *d* type, while for higher frequencies $\omega > \omega_0$, the wave acquires a left-handed polarization and the isomer is of the *l* type. From Fig. 4(b) it is also evident that the transmitted wave passes through a linearly polarized state ($\delta=0$) at the fundamental frequency $\omega_0=66.7$ THz. Despite the energy dissipation in the metal, over 40% of the incident energy is transmitted around the resonance frequency.

In Fig. 4, we have calculated the amplitude and phase change of the transmitted wave for the configuration in Fig. 1(a). Another configuration is also considered in our simulations, in which the first and second SSRRs exchange their places. For *y*-polarized incident wave, the first SSRR is turned with its slit in the “wrong” position for the incident *E* field and the second “correctly” for that incident field.²⁸ In this case $|E_y|$ still appears to have a Lorentz line shape. How-

ever, as the two SRRs exchange their places, the phase difference $\delta=\delta_y-\delta_x$ alters its sign. This effect is due to the absence of inversion-invariance in our 3D chiral structure.

In general, the principal axes of the ellipse described by Eq. (3) are not aligned with the *x* and *y* directions. The angle θ between the major polarization axis and \hat{y} [see Fig. 1(b)] can be calculated from the equation $\tan 2\theta = 2|E_x||E_y|\cos \delta/(|E_x|^2-|E_y|^2)$,²⁷ with the numerically obtained result shown in Fig. 4(b). A distinctive, bell-type shape is observed with θ reaching a maximum value 156.7° at $\omega_m=68.4$ THz. Although $\cos \delta$ reaches a maximum at ω_0 , the angle θ optimizes at $\omega_m \neq \omega_0$ due to the frequency dependence of the electric field amplitudes. At frequencies 62.5 THz and 74.6 THz, one has $\theta=90^\circ$ and the major axes of the wave polarization coincides with the *x* or *y* spatial directions, respectively. A detail schematics showing all polarization states that can be acquired by the transmitted wave is depicted in Fig. 4(c). Additionally, an animation of the change in polarization is accessible online.²⁸

In conclusion, we propose a magnetic plasmon dimer (MD) made of single split ring resonators showing a magnetic response at infrared frequencies. The resonance properties of the MD are successfully described by a quasimolecular hybridization model. A split in the system resonance is observed due to inductive interaction, which strongly depends on the separation distance between the resonators. Under conditions of strong magnetic coupling, optical activity is demonstrated at near-infrared frequencies. A linearly polarized light flips into an elliptically polarized state when it passes through a periodic array of MDs. Thus, an artificial chiral metamaterial made of a large number of resonators could be utilized to tune the polarization of an incident light over a wide range of angles. Optical elements, such as tunable polarizers and switches, are possible applications of the proposed MD based complex media.

This work was supported by AFOSR MURI (Grant No. FA9550-04-1-0434), SINAM, and NSEC under Contract No. DMI-0327077.

*Corresponding author. xiang@berkeley.edu

¹J. B. Pendry *et al.*, IEEE Trans. Microwave Theory Tech. **47**, 2075 (1999).
²R. Marques *et al.*, J. Opt. A, Pure Appl. Opt. **7**, S38 (2005).
³D. R. Smith *et al.*, Phys. Rev. Lett. **84**, 4184 (2000).
⁴R. A. Shelby, D. R. Smith, and S. Schultz, Science **292**, 77 (2001).
⁵I. Tinoco and M. P. Freeman, J. Phys. Chem. **61**, 1196 (1957).
⁶J. B. Pendry, Science **306**, 1353 (2004).
⁷A. Papakostas *et al.*, Phys. Rev. Lett. **90**, 107404 (2003).
⁸A. V. Rogacheva *et al.*, Phys. Rev. Lett. **97**, 177401 (2006).
⁹V. P. Drachev *et al.*, J. Opt. Soc. Am. B **18**, 1896 (2001).
¹⁰T. J. Yen *et al.*, Science **303**, 1494 (2004).
¹¹S. Linden *et al.*, Science **306**, 1351 (2004).
¹²N. Katsarakis *et al.*, Opt. Lett. **30**, 1348 (2005).
¹³C. Enkrich *et al.*, Phys. Rev. Lett. **95**, 203901 (2005).
¹⁴J. Zhou *et al.*, Phys. Rev. Lett. **95**, 223902 (2005).
¹⁵A. Ishikawa, T. Tanaka, and S. Kawata, Phys. Rev. Lett. **95**, 237401 (2005).

¹⁶T. Tanaka, A. Ishikawa, and S. Kawata, Phys. Rev. B **73**, 125423 (2006).
¹⁷H. Liu *et al.*, Phys. Rev. Lett. **97**, 243902 (2006).
¹⁸E. Prodan *et al.*, Science **302**, 419 (2003).
¹⁹E. Prodan and P. Nordlander, J. Chem. Phys. **120**, 5444 (2004).
²⁰P. Nordlander *et al.*, Nano Lett. **4**, 899 (2004).
²¹D. W. Brandl, C. Ouber, and P. Nordlander, J. Chem. Phys. **123**, 024701 (2004).
²²C. Ouber and P. Nordlander, J. Phys. Chem. B **109**, 10042 (2005).
²³P. Nordlander and E. Prodan, Nano Lett. **4**, 2209 (2004).
²⁴F. Le *et al.*, Nano Lett. **5**, 2009 (2005).
²⁵M. A. Ordal *et al.*, Appl. Opt. **22**, 1099 (1983).
²⁶E. U. Condon, Rev. Mod. Phys. **9**, 432 (1937).
²⁷J. D. Jackson, *Classical Electrodynamics* (Wiley, NY, 1999).
²⁸EPAPS Document No. E-PRBMDO-76-041731 for supplementary material. For more information on EPAPS, see <http://www.aip.org/pubservs/epaps.html>.